PHYSICAL REVIEW B **72**, 054208 (2005)

Doping, density of states, and conductivity in polypyrrole and poly(*p*-phenylene vinylene)

I. N. Hulea,[1,2] H. B. Brom,[1] A. K. Mukherjee,[3] and R. Menon[3]
[1]*Kamerlingh Onnes Laboratory, Leiden University, P. O. Box 9504, 2300 RA Leiden, The Netherlands*
[2]*Dutch Polymer Institute (DPI), P. O. Box 902, 5600 AX Eindhoven, The Netherlands*
[3]*Department of Physics, Indian Institute of Science, Bangalore, India*
(Received 9 December 2004; revised manuscript received 15 June 2005; published 19 August 2005)

The evolution of the density of states (DOS) and conductivity as a function of well-controlled doping levels in OC_1C_{10}-poly(*p*-phenylene vinylene) [OC_1C_{10}-PPV] doped by $FeCl_3$ and PF_6, and PF_6-doped polypyrrole (PPy-PF_6), has been investigated. At a doping level as high as 0.2 holes per monomer, the former one remains nonmetallic while the latter crosses the metal-insulator transition. In both systems, a similar almost linear increase in DOS as a function of charges per unit volume (c^*) has been observed from the electrochemical gated transistor data. In PPy-PF_6, when compared to doped OC_1C_{10}-PPV, the energy states filled at low doping are closer to the vacuum level; by the higher c^* at high doping, more energy states are available, which apparently enables the conduction to change to metallic. Although both systems on the insulating side show $\log \sigma \propto T^{-1/4}$ as in variable range hopping, for highly doped PPy-PF_6 the usual interpretation of the hopping parameters leads to seemingly too high values for the density of states.

DOI: 10.1103/PhysRevB.72.054208 PACS number(s): 71.20.Rv, 72.80.Le, 72.20.Ee, 73.61.Ph

I. INTRODUCTION

Since the discovery of conducting polyacetylene (PAc) at the end of the 1970s,[1] charge-transport mechanisms in semiconducting and conducting polymers have been of great interest. In polypyrrole (PPy), as in PAc, a transition from insulating (zero dc conductance for temperature T going to zero) to metallic state (nonzero dc conductance in the limit of zero Kelvin) occurs by increasing the doping level,[2] and metallic PPy, among highly doped conducting polymers, is one of the most widely studied due to its environmental stability, which makes it attractive for technological applications. Usually in conducting polymers, doping adds or removes electrons to the π band formed by the overlapping p orbitals in the conjugated polymer backbone. Although the electrons in the π band could be delocalized, not all conjugated polymers can be brought into the metallic state. For example, polyalkylthiophenes (PAT) and poly[2-methoxy-5-(3′,7′-dimethyloctyloxy)-*p*-phenylene vinylene] (OC_1C_{10}-PPV),[3] that have been frequently used in polymeric transistors and polymeric light-emitting diodes, respectively, remain as insulators even at the highest doping levels (with dopants like $FeCl_3$).[4–6]

To explain the transport data in conducting polymers in general, key ingredients are the crystalline coherence length (a few nanometers), the volume fraction of crystallinity (>50%), the doping level, the interchain transfer integral, the energy dependence of the density of states, the extent of disorder in the material, charge repulsion, and polaronic effects.[7–11] The relevant values of the transfer integral, the spread in its mean value due to disorder, and the Coulomb correlations are usually all around 0.1 eV or less, which is close to the thermal energy at 300 K. A systematic study of the evolution of the density of states (DOS) and charge transport as a function of well-controlled doping level is still lacking in several conducting polymers. In this work, the difference between $FeCl_3$ and PF_6-doped OC_1C_{10}-PPV and PF_6-doped PPy, as a function of doping level, is investigated in detail by studying both the electrochemical gated transistor (EGT) characteristics and temperature dependence of conductivity using a precise calibration of the amounts of doping. The higher DOS per unit volume for PF_6-doped PPy compared to doped OC_1C_{10}-PPV and the occupation of the energy states near the Fermi level explain the observed difference in conductivity behavior.

II. EXPERIMENT

OC_1C_{10}-PPV was doped in solution with iron(III)chloride, $FeCl_3$. Ideally, the following redox reaction should take place: $PPV + 2FeCl_3 \rightarrow PPV^+ + FeCl_2 + FeCl_4^-$. Films were obtained by slowly evaporating the solvent.[4] Under ambient conditions, the conductive properties of the films were stable over several weeks. Polypyrrole doped by PF_6 (PPy-PF_6) was polymerized and doped by anodic oxidation in an electrochemical cell with glassy carbon electrode and platinum foil as working and counterelectrodes, respectively. The polymerization was carried out at −40 °C under nitrogen atmosphere to improve the structural order in the system, and the samples were systematically dedoped to attain the desired doping level.[12,13] Free-standing films (thickness ~20 μm) were used for conductivity measurements, and the films on the glass substrate, on which Au contacts were evaporated before deposition, were used for electrochemical gated transistor (EGT) experiments. In the EGT measurements on PPV and PPy, the hole charge was counterbalanced by PF_6^- anions from the electrolyte solution.[14]

III. RESULTS AND DISCUSSION

A. Doping level and density of states

The $FeCl_3$ doping levels in the PPV samples used for the T dependence of σ were calculated from the amount of chemicals used in the solutions, and further investigated in

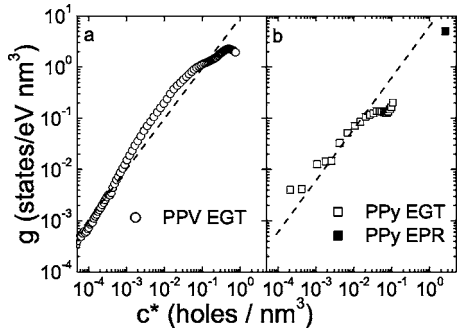

FIG. 1. g vs c^* on a double log scale. (a) EGT data for PF_6-doped PPV. The found dependence is roughly linear at low doping. The dashed line corresponds to $g \propto c^*$. (b) PF_6-doped PPy from EGT and ESR (at $c^*=2.54$ charges per nm^3) data (Ref. 16). The found dependence is again almost linear (dashed line) at low doping.

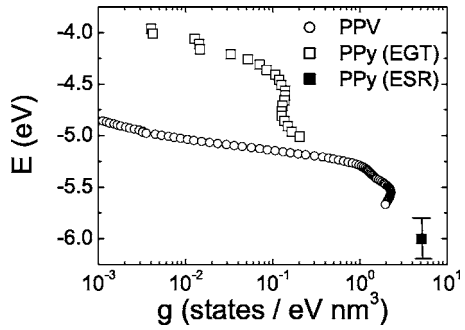

FIG. 2. The E dependence of the experimentally determined DOS of PPy (per eV and nm^3) compared to PPV on a linear-log scale (Ref. 14). Due to chemical instability of PPy in the EGT, no data points at high doping levels are available.

detail by Fe Mössbauer measurements.[6] The doping levels discussed in this work are between 0.02 and 0.33 charges per monomer (c). Also, earlier studies have shown that by using the semiconducting polymer in an EGT, c can be obtained by summing the integrated currents, which are directly measured as described below; c ranges from 10^{-4} up to 0.4. The PF_6 levels in the PPy samples in the T dependence of σ data were deduced from ^{19}F-NMR and by using the sum rule for $\sigma(\omega)$ too (for details, see Appendix I); c lies between 0.065 and 0.23. In PPy-EGT, the c values discussed here range between 10^{-4} and 10^{-2} charges per monomer; at higher doping levels, the measurements were not reversible and reproducible. Doping levels can also be expressed per nm^3 (c^*), by knowing the estimated volume of a monomer (ring volume), which in PPy is 0.13 nm^3 and in PPV is 0.48 nm^3.[15] The latter convention will be used in the following.

The density of states will be expressed as the number of states per eV per nm^3, and is denoted by g. In an EGT study, g is determined as a function of energy. It equals the number of elementary charges $\Delta Q/e$ that can be stored in the polymer in a small step of the electrochemical potential (μ_e) of $\approx$10 meV, divided by the number of monomers and the monomer volume. This number can be easily calculated. The concentration at a given voltage is obtained via summation of all $\Delta Q/e$ up to that value. The g versus c^* data for PF_6-doped PPV are shown in Fig. 1(a). The data follow a linear dependence $g \propto c^*$ (the dashed line), especially at lower doping levels. Because $dc^*/d\mu_e = g(\mu_e)$, it means that $g \propto \exp(\mu_e)$ up to 0.5 states per eV per nm^3. At higher values of $g(E)$, the dependence on E becomes Gaussian, as shown in previous work.[14] The g versus c^* data for PF_6-doped PPy are shown in Fig. 1(b). The EGT data are almost linear in c^*, and stable only at low PF_6 concentrations. To extrapolate the behavior of g versus c^*, the data point at high doping level $c^*=2.54$, from an ESR study by Joo *et al.*,[16] is included. From the same ESR study, the DOS at the Fermi level per spin was determined to be 0.33 states/(eV monomer) for a metallic sample of PF_6-doped PPy.

A comparison of E versus g in both systems is shown in Fig. 2. Knowing the Ag reference electrode location at 4.47 V below the vacuum level, the electrochemical potentials could be correlated with the vacuum level.[14] Based on the EGT data with the additional data point from ESR, the tail of the distribution of the hole states (at doping levels below 1%) in PPy-PF_6 is seen to be wider than in PPV, and also the maximum in $g(E)$ is higher. However, a full comparison is hindered by the absence of reliable PPy data from EGT above 0.2 states/nm^3 eV.

B. Conductivity

The conductivity σ versus $T^{-1/4}$ at various doping levels is shown in Fig. 3 in logarithmic-linear scale. In both systems, the T dependence of σ is quite sensitive to c. The most noticeable difference among PPV and PPy is that σ of PPy-PF_6 for $c>0.16$ follows a real metallic T dependence (large finite σ as $T \to 0$ K), whereas even in fully doped OC_1C_{10}-PPV, σ still decreases by several orders of magnitude with T. Furthermore, in both systems the equation $\sigma(T)=\sigma_0 \exp[-(T_0/T)^{1/4}]$, expected for three-dimensional (3D) variable range hopping (VRH),[17] fits the data quite well for almost all values of doping, especially at low temperatures. In the usual analysis, T_0 is connected to the density of

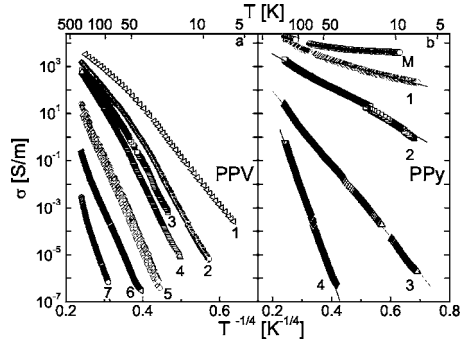

FIG. 3. $\sigma(T)$ vs $T^{-1/4}$ for $FeCl_3$-doped PPV (a) and PPy-PF_6 (b) on a logarithmic-linear scale. At low T, $\sigma(T)=\sigma_0 \exp[-(T_0/T)^{1/4}]$; the lines are fits used to determine T_0. (a) The doping levels per monomer (per nm^3) of the samples 1 to 7 are, respectively, 0.33 (0.69), 0.17 (0.36), 0.10 (0.21), 0.08 (0.17), 0.06 (0.13), 0.03 (0.06), and 0.02 (0.04). (b) The doping levels per monomer (per nm^3) of the metallic sample M and the insulating samples 1 to 4 are 0.23 (1.82), 0.16 (1.22), 0.14 (1.14), 0.075 (0.57), and 0.065 (0.51).

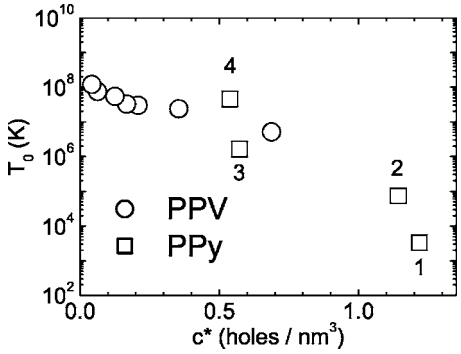

FIG. 4. T_0 vs c^* for both $FeCl_3$-doped PPV (see Ref. 6) and PF_6-doped PPy. T_0 is determined from the $T^{-1/4}$-dependence of log σ; see Fig. 3.

states g via $k_B T_0(c) \sim 20\alpha^3/g(E)$.[18] The parameter α^{-1} characterizes the decay of the squared wave function away from the localization site and equals 0.2 - 0.4 nm.[18] For doped PPV, the T_0 method gives reliable results for the DOS in the VRH regime at low temperatures (around 1 state per eV and nm^3, in agreement with the EGT data). For PPV, the analysis could be extended by taking into account that at higher doping levels, the size of the delocalized regions increases.[6] However, for the two highest doped samples of PPy, the values for the DOS determined from T_0 (10^2–10^3 states per eV and nm^3) are orders of magnitude higher (note the logarithmic vertical scale in Fig. 4) than the ones determined for PPV or measured by the EGT method. Even by allowing a growing size of the delocalized region,[6] no reasonable g values could be obtained. Apparently, the particular character of the disorder in the polymeric material close to the metal-insulator transition (see Refs. 7–9 and 11) requires a more sophisticated analysis of the T_0 parameter.

IV. CONCLUSIONS

The DOS per monomer volume as a function of energy at very precise values of doping levels in both OC_1C_{10}-PPV doped with $FeCl_3$ and PF_6, and PF_6-doped PPy, has been determined. An almost linear increase in DOS versus c^* has been observed in both systems from the EGT data. For PF_6-doped PPy at high c^*, the DOS per monomer volume is higher and states closer to the center of the band can be populated, which eventually can make the polymer metallic (other parameters like the interchain transfer integrals remain, of course, essential in charge transport). This study has also shown that, while for doped PPV interpretation of the data within a VRH picture works well, for highly doped PF_6-PPy such an interpretation might lead to too high estimates of the density of states.

ACKNOWLEDGMENTS

We acknowledge fruitful discussions with Reinder Coehoorn and Hubert Martens (Philips Research) and Frank Pasveer and Thijs Michels (Technical University of Eindhoven and Dutch Polymer Institute). Arjan Houtepen (University of Utrecht) helped us to perform the measurements with the electrochemical transistor and Oleg Bakharev (Leiden University) helped with the NMR spectrometer. This work forms part of the research program of the Dutch Polymer Institute (DPI), project DPI274.

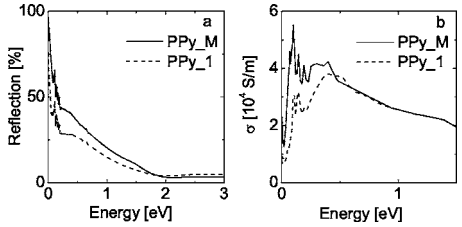

FIG. 5. (a) IR and UV/VIS reflection of two PF_6-doped PPy samples at 300 K. The overall features are similar. (b) The real part of the conductivity $\sigma(\omega)$ derived from (a) according to the procedure in the text. Via the optical sum rule, the real part of $\sigma(\omega)$ or the imaginary component of the dielectric constant $\epsilon(\omega)$ is related to the number of carriers.

APPENDIX A: THE DOPING LEVEL

The PF_6 doping levels were determined by use of the optical sum rule and NMR. Below, we explain why we preferred the outcome of the NMR analysis.

Optical sum rule

Romijn *et al.* used reflection data in the range 5 meV–3.5 eV together with the boundary conditions set by phase-sensitive sub-THz spectroscopy to calculate the phase via the Kramers-Kronig relation $\{\theta(\omega_0) = \omega_0/2\pi \int_0^\infty \ln[R(\omega)/R(\omega_0)]/[\omega_0^2 - \omega^2] d\omega\}$.[8] The reflection amplitude and phase give the real and imaginary parts of the dielectric constant, see Fig. 5, where the imaginary component of the complex relative dielectric constant $\epsilon_2(\omega)$ [or the real part of the conductivity $\sigma(\omega) = \omega\epsilon_0\epsilon_2(\omega)$ with ϵ_0 the vacuum dielectric constant] is related to the number of carriers via the sum rule[8,13]

$$\frac{N_h(E)}{m^*} = \frac{2\epsilon_0}{\pi e^2} \int_0^E \omega\epsilon_2(\omega) d\omega. \tag{A1}$$

In this way, the ratio $N_h(E)/m^*$ was determined with $N_h(E)$ the number of carriers per m^3 and m^* their effective mass. By making an additional assumption about the effective mass, the number of carriers was estimated. For m^* equal to the free-electron mass, the number of carriers for PPy_M found by Romijn *et al.* was about 3 holes/nm^3.[8]

We collected reflection data on PPy samples with very different room-temperature dc conductivities. The outcome of the sum rule is somewhat arbitrary, because at energies of ($\sim$3 eV) intraband excitations start playing a role as well.[13,19] By integrating the conductivity up to 3.2 eV, the results show that in PPy_4 (notation as in Fig. 3), a carrier density of 2 holes/nm^3 is present, while for PPy_1 (see also Fig. 5) the carrier density equals 3 holes/nm^3; hence the values of carrier densities in all measured samples are rather close, though their $\sigma(T)$'s are widely different.

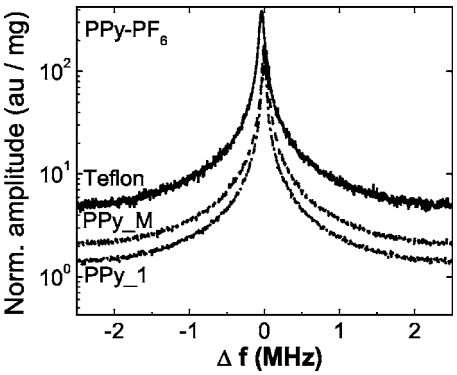

FIG. 6. ^{19}F signal normalized to the sample mass (background subtracted) as a function of frequency difference with the central frequency 376.302 MHz. Shown are Fourier transforms of free induction decays for teflon, the metallic sample PPy_*M*, and sample PPy_1 (other samples are omitted for clarity).

NMR

A more accurate way to measure the amount of doping is by nuclear magnetic resonance experiment (NMR). None of the atomic species present in the dopant (PF_6) are contained in PPy. Because for each P atom there are six F atoms and F has spin $I=1/2$ with a very large nuclear magnetic moment, we monitored the F atoms in 9.4 T at a frequency of 376.302 MHz via the free induction decay (FID). In Fig. 6, the signals normalized to the sample mass of two samples and a teflon (building block C_2F_4) reference are plotted. The F intensity for each of the samples is obtained by integration of the signal. The similarity in line shapes of all F-lines allowed the integration to be cut off at the border of the figure without affecting the intensity ratios.

Because the signal intensity I^S is proportional to the number of F atoms in the samples, the doping levels per monomer $c=n_{\mathrm{PF}_6}/n_{\mathrm{PPy}}$ can be easily determined,

$$c=\left(\frac{m_{\mathrm{PPy}}}{m_{\mathrm{PF}_6}}\right)\times\left(\frac{6M^S}{4M^T}\frac{I^T}{I^S}\frac{m_{\mathrm{C_2F_4}}}{m_{\mathrm{PF}_6}}-1\right)^{-1}, \qquad \text{(A2)}$$

where the PPy mass equals the monomer mass (m_{PPy}) times the number of monomers (n_{PPy}), the PF_6 mass is the number of ions (n_{PF_6}) multiplied with the ion mass (m_{PF_6}), and the sample mass $M^S=m_{\mathrm{PPY}}n_{\mathrm{PPy}}+m_{\mathrm{PF}_6}n_{\mathrm{PF}_6}$. M^T and I^T denote, respectively, the teflon mass and signal intensity. For samples *M*, 1, and 4, the determined doping concentrations were, respectively, 0.23 ± 0.2, 0.16 ± 0.02, and 0.065 ± 0.01 in units of holes/monomer. From the NMR analysis, the insulating sample no. 4 appears to be almost three times lower doped than the metallic sample *M*, which is more realistic than the values obtained from the optical sum rule.

[1] C. K. Chiang, C. R. Fincher, Y. W. Park, A. J. Heeger, H. Shirakawa, E. J. Louis, S. C. Gau, and A. G. MacDiarmid, Phys. Rev. Lett. **39**, 1098 (1977).
[2] H. C. F. Martens, H. B. Brom, and R. Menon, Phys. Rev. B **64**, 201102(R) (2001) and **65**, 079901(E) (2002).
[3] PPV, when streched and without sidechains, can be brought into the metallic state by doping with, e.g., H_2SO_4, see M. Ahlskog, R. Menon, A. J. Heeger, T. Noguchi, and T. Ohnishi, Phys. Rev. B **53**, 15529 (1996).
[4] J. A. Reedijk, H. C. F. Martens, H. B. Brom, and M. A. J. Michels, Phys. Rev. Lett. **83**, 3904 (1999).
[5] I. G. Romijn, W. F. Pasveer, H. C. F. Martens, H. B. Brom, and M. A. J. Michels, Synth. Met. **119**, 439 (2001).
[6] H. C. F. Martens, I. N. Hulea, I. Romijn, H. B. Brom, W. F. Pasveer, and M. A. J. Michels, Phys. Rev. B **67**, 121203(R) (2003).
[7] V. N. Prigodin, A. N. Samukhin, and A. J. Epstein, Synth. Met. **141**, 155 (2004).
[8] I. G. Romijn, H. J. Hupkes, H. C. F. Martens, H. B. Brom, A. K. Mukherjee, and R. Menon, Phys. Rev. Lett. **90**, 176602 (2003).
[9] H. C. F. Martens and H. B. Brom, Phys. Rev. B **70**, 241201(R) (2004).
[10] R. S. Kohlman, A. Zibold, D. B. Tanner, G. G. Ihas, T. Ishiguro, Y. G. Min, A. G. MacDiarmid, and A. J. Epstein, Phys. Rev. Lett. **78**, 3915 (1997).
[11] A. B. Kaiser, Adv. Mater. (Weinheim, Ger.) **13**, 927 (2001) and Rep. Prog. Phys. **64**, 1 (2001).
[12] C. O. Yoon, M. Reghu, D. Moses, and A. J. Heeger, Phys. Rev. B **49**, 10851 (1994).
[13] K. Lee, R. Menon, C. O. Yoon, and A. J. Heeger, Phys. Rev. B **52**, 4779 (1995).
[14] I. N. Hulea, H. B. Brom, A. J. Houtepen, D. Vanmaekelbergh, J. J. Kelly, and E. A. Meulenkamp, Phys. Rev. Lett. **93**, 166601 (2004).
[15] J. P. Pouget, Z. Oblakowski, Y. Nogami, P. A. Albouy, M. Laridjani, E. J. Oh, Y. Min, A. G. MacDiarmid, J. Tsukamoto, T. Ishiguro, and A. J. Epstein, Synth. Met. **65**, 131 (1994).
[16] J. Joo, J. K. Lee, S. Y. Lee, K. S. Jang, E. J. Oh, and A. J. Epstein, Macromolecules **33**, 5131 (2000).
[17] N. F. Mott, Philos. Mag. **19**, 835 (1969).
[18] H. Böttger and V. V. Bryksin, *Hopping Conduction in Solids* (Akademie-Verlag Berlin, 1985).
[19] H. J. Lee and S. M. Park, J. Phys. Chem. B **108**, 1590 (2004).